CO$_2$ Mineralization Using Brine Discharged from a Seawater Desalination Plant

Jun-Hwan Bang, Yeongsuk Yoo, Seung-Woo Lee, Kyungsun Song and Soochun Chae *

Change Mitigation and Sustainability Division, Korea Institute of Geoscience and Mineral Resources (KIGAM), 124 Gwahang-no, Yuseong-gu, Daejeon 34132, Korea; jhbang@kigam.re.kr (J.-H.B.); ysyoo6804@kigam.re.kr (Y.Y.); swlee21th@kigam.re.kr (S.-W.L.); kssong@kigam.re.kr (K.S.)
* Correspondence: chae@kigam.re.kr

Abstract: CO$_2$ mineralization is a method of sequestering CO$_2$ in the form of carbonated minerals. Brine discharged from seawater desalination is a potential source of Mg and Ca, which can precipitate CO$_2$ as forms of their carbonate minerals. The concentration of Mg and Ca in brine are twice those in the seawater influent to desalination process. This study used a cycle for CO$_2$ mineralization that involves an increase in the pH of the brine, followed by CO$_2$ bubbling, and, finally, filtration. To the best of our knowledge, this is the first time that non-synthesized brine from a seawater desalination plant has been used for CO$_2$ mineralization. The resulting precipitates were CaCO$_3$ (calcite), Mg$_5$(CO$_3$)$_4$(OH)$_2$·4H$_2$O (hydromagnesite), and NaCl (halite) with these materials being identified by X-ray Diffraction (XRD), Fourier transform infrared (FTIR) and thermo gravimetric-differentail thermal Analysis (TGA)-DTA. Despite the presence of Ca with Mg in brine being unfavorable for the precipitation of Mg carbonate, Mg reacted with CO$_2$ to form hydromagnesite at a yield of 86%. Most of the Ca formed calcite, at 99% yield. This study empirically demonstrates that brine from seawater desalination plants can be used for CO$_2$ mineralization.

Keywords: CO$_2$ mineralization; desalination; carbonates; brine; seawater

1. Introduction

Climate change and abnormal weather phenomena have been worsening, owing to increased CO$_2$ emissions around the world. Typically, the Korean peninsula is not a region that is known to suffer from water shortages [1]. However, since in the last few years there have been severe annual droughts, especially in west-coast areas, with increased CO$_2$ emissions being blamed. Several methods of preserving water resources have been examined, and seawater desalination has been found to be a successful candidate [2,3]. Seawater desalination processes remove the salts from seawater by distillation, membrane separation, and/or reverse osmosis (RO) to produce useful water that is suitable for drinking and industrial purposes [3–5]. One result of these processes is that concentrated seawater (i.e., brine) is also produced, in which the rejected salts in seawater have been concentrated. Desalination consumes large amounts of energy, meaning that large-scale desalination plants are often placed near power stations [2], and also leads to the emission of massive amounts of CO$_2$, which will eventually exacerbate the problems that desalination is attempting to solve. Methods of limiting CO$_2$ emissions or removing CO$_2$ from desalination plants are, therefore, of great interest.

CO$_2$ mineralization is one such method of sequestering CO$_2$. In this method, CO$_2$ reacts with calcium and/or magnesium to form calcium carbonate and/or magnesium carbonate [6]. The rate of CO$_2$ mineralization can be accelerated when the reaction takes place in the aqueous phase, as happens in typical chemical reactions. Ionization of CO$_2$ to CO$_3{}^{2-}$ takes place under alkaline conditions. This is essential for CO$_2$ mineralization, as it allows ionic reactions between CO$_3{}^{2-}$ and Ca^{2+} and/or Mg^{2+}.

For this reason, alkaline chemicals such as NaOH or NH_4OH are applied to increase the pH of the aqueous phase in CO_2 mineralization [7,8].

Meanwhile, using Ca and Mg from industrial waste such as waste concrete, slags from steel production, and liquid wastes is preferable when attempting to design feasible CO_2 mineralization processes [9–13]. Detailed principles and applications of CO_2 mineralization using alkaline waste have been summarized by Pan et al. [14]. Some pretreatment steps, such as crushing, sieving, activation, and/or digestion are required to extract Ca and Mg from solid waste [13,15,16]. When using liquid waste, such pretreatment procedures are not required because the Ca and/or Mg are already present as ions. For this reason, the use of brine for CO_2 mineralization is a promising route for investigation [6,8,17]. In the implementation of this technology, both engineering and economic factors are important, as is environmentally balanced performance [18].

It is reported that the concentrations of the rejected salts in brine from desalination plants using reverse osmosis (RO) systems are 2–2.5 times higher than those in influent seawater [19], suggesting that brine could be a promising material for CO_2 mineralization. If Mg alone is present in a solution, it readily reacts with CO_2 to precipitate Mg carbonates; the reaction between $MgCl_2 \cdot 6H_2O$ solution and CO_2 produced nesquehonite ($MgCO_3 \cdot 3H_2O$), dypingite ($Mg_5(CO_3)_4(OH)_2 \cdot 5H_2O$), dypingite-like ($Mg_5(CO_3)_4(OH)_2 \cdot 8H_2O$), and hydromagnesite ($Mg_5(CO_3)_4(OH)_2 \cdot 4H_2O$) crystal phases, depending on the reaction conditions [20]. When considering brine for CO_2 mineralization, it is worth noting that in previously reported studies, materials in a replica brine solution with coexisting Mg and Ca were not readily carbonated. Liu and Maroto-Valer [21] synthesized oil-field brine and conducted CO_2 mineralization experiments under mimicked underground conditions to precipitate calcite. An artificial brine containing metal ions such as Na^+, Mg^{2+}, Ca^{2+}, K^+, and Sr^{2+}, and anions including Cl^-, SO_4^{2-}, Br^-, BO_3^{3-}, F^-, and HCO_3^- was unfavorable for the precipitation of Mg carbonates, but was favorable for $CaCO_3$ precipitation [22]. In the same manner, simulated brine composed of NaCl, $MgCl_2$, $CaCl_2$, Na_2SO_4, and KCl precipitated $CaCO_3$ by the primary separation of $Mg(OH)_2$ from the Ca^{2+} solution [23]. Owing to the significantly higher concentration of Mg than Ca in seawater and brine, Mg would allow much more CO_2 mineralization than Ca does. However, this does not necessarily mean that more precipitating Mg carbonates than Ca carbonates will be produced, because Ca carbonates are more sparingly soluble than Mg carbonates (for example, $K_{sp \, (hydromagnesite)} = 1.26 \times 10^{-5}$ [24], and $K_{sp \, (calcite)} = 3.36 \times 10^{-9}$ at 25 °C each [25]).

This paper introduces the first use of non-synthesized brine discharged from a functional seawater desalination plant for CO_2 mineralization; we have particularly focused on the precipitation of Mg carbonates. Repeated cycles involved the pH adjustment of brine, and the injection of CO_2 microbubbles showed that Mg carbonation could be achieved alongside Ca. Various analytical techniques were used for the identification of the precipitates, including X-ray diffraction (XRD) analysis. We have empirically proved that CO_2 mineralization using brine for CO_2 sequestration.

2. Experimental

The brine used in this study was collected from an ongoing seawater RO process for industrial water supplementation in Korea. The major cations and anions in this brine and their concentrations as measured by inductively coupled plasma atomic emission spectroscopy (ICP-OES; Optima 8300, PerkinElmer, Shelton, CT, USA) are listed in Table 1. The concentrations of Sr, Si, Li, Cu, and rare earth elements such as W, Mo, and Rb were also measured, but the values obtained were not significant. Anion concentrations were measured by ion chromatography (IC; Dionex ICS-5000+, Thermo Fisher Scientific, Sunnyvale, CA, USA), and the SO_4^{2-} concentration was measured using IC equipped with an Ag cartridge (Dionex OnGuard II Ag, Thermo Fisher Scientific).

Table 1. Concentrations of the major cations and anions in the brine.

Ions	Mg	Ca	Na	K	Cl	SO_4
Concentration (mg/L)	2226	714	17,987	858	32,220	4766

NaOH solution (1 M) was prepared for use as an alkaline chemical by dilution of NaOH (96%, Junsei Chemicals, Tokyo, Japan) with deionized water (Milli-Q Gradient-A10, Millipore, Billerica, MA, USA). The pH of 0.25 L of brine was increased from an initial value of 8.2 to 10–13.5 (measured by Orion Star A215, Thermo Scientific, Singapore) by adding the 1 M NaOH solution to the brine in a beaker with a lid at a rate of 4 mL/min using a peristaltic pump (EMP-2000W, EMS-tech, GyeongGi, Korea) at ambient temperature and pressure. The brine was stirred while the NaOH solution was added, and as the pH of the brine increased, a suspension of white precipitates was formed. Once the target pH was reached, the suspension was filtered with a 0.45 μm pore nylon membrane (Whatman, Brentford, UK) to allow the concentrations of the metal ions listed in Table 1 to be measured by ICP-OES. However, only the concentrations of Mg, Ca, and Na changed with pH and, as such, only the concentrations of these three elements are reported in the results section.

In the cyclic CO_2 mineralization experiments, as 1 L of brine reached pH 10.5, we reacted the suspension with CO_2 (99%, Gasco) instantly, and monitored for further pH changes at atmospheric pressure. A jacket reactor was used for CO_2 mineralization, with a coolant at 1 °C being circulated between the walls by a chiller, and a lid being placed on the upper part of the reactor. As CO_2 microbubbles were injected into the suspension using a microbubble generator, the pH decreased rapidly, as has already been shown in the literature [7,26,27]. CO_2 injection was stopped once the pH of the brine had decreased to 8. This was because we found that we were unable to collect the CO_2-reacted precipitates when CO_2 injection was stopped at pH 7, which was the value we had used in previous studies [7,26]. The final products, which consisted of precipitates and transparent solutions, were obtained by filtering the brine through a 0.45 μm nylon filter. The experimental cycle was then begun again, with the pH of the solution being increased to 10.5, CO_2 bubbling taking place, and the precipitate formed being filtered off. This cycle was repeated until no precipitates were obtained on addition of NaOH, which occurred during the 5th cycle. This indicated that there were no divalent ions such as Mg or Ca that were able to form hydroxides; thus, CO_2 bubbling did not lead to the formation of particles. Therefore, in our experiment, four cycles were sufficient to remove all divalent ions from the brine through the formation of particles. The experimental cycle is shown in Figure 1. We decided not to consider the effect of dissolved CO_2 from atmosphere during the experiments, because we believed that Mg^{2+}, which was 3 times more abundant than Ca^{2+} in the brine, would not be carbonated by atmospheric CO_2 under the experimental conditions.
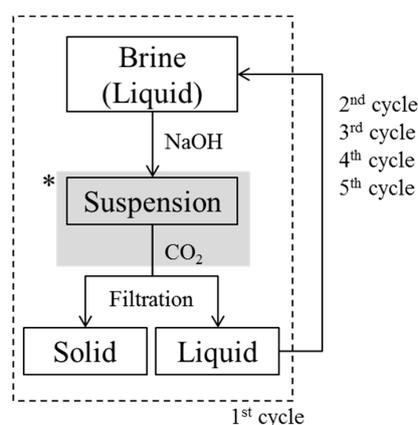
* CO_2 mineralization occurs in the marked block ▨.

Figure 1. Experimental cycles showing increase in pH, CO_2 injection, and filtration after CO_2 mineralization.

After the reaction with CO_2, the suspension was filtered, the concentrations of Mg, Ca, and Na in the filtered liquid samples were analyzed, and the filter cake was dried in an oven at 80 °C for 24 h, then characterized using XRD (X'pert MPD, Philips, EA Almelo, The Netherlands), a field emission scanning electron microscope (FESEM; JSM-7800 FPRIME, JEOL, Tokyo, Japan) equipped with an energy dispersive spectrometer (EDS; X-MaxN, Oxford), thermogravimetric analysis (TGA; DTG-60H, Shimadzu, Kyoto, Japan) at argon environment (10 °C/min heating rate), and Fourier transform infrared spectroscopy (FTIR; NICOLET 380, Thermo Fisher Scientific Inc., Costa Mesa, CA, USA).

3. Results and discussion

3.1. Concentrations of Mg, Ca, and Na in Brine with Different pH Values

Initial experiments aimed to obtain information on the changes in the concentrations of Mg and Ca as the pH was varied from 10–13.5 by adding NaOH solution to brine. This resulted in the formation of a white suspension. The suspension thickened as the amount of NaOH solution added increased. ICP-OES was used to measure the concentrations of the ions; the results are shown in Figure 2. The label "raw" on the horizontal axis represents the untreated brine (i.e., no NaOH solution had been added). The left vertical axis shows the concentrations of Mg and Ca, while the right vertical axis shows the concentration of Na. It can be seen that the concentrations of Mg and Ca were reproducible; however, the concentration of Na showed large standard deviations because the solutions were prepared for ICP-OES measurement by diluting them by a factor of 1000. It was expected that the concentration of Na would increase as the pH increased, owing to the addition of NaOH solution to the brine.
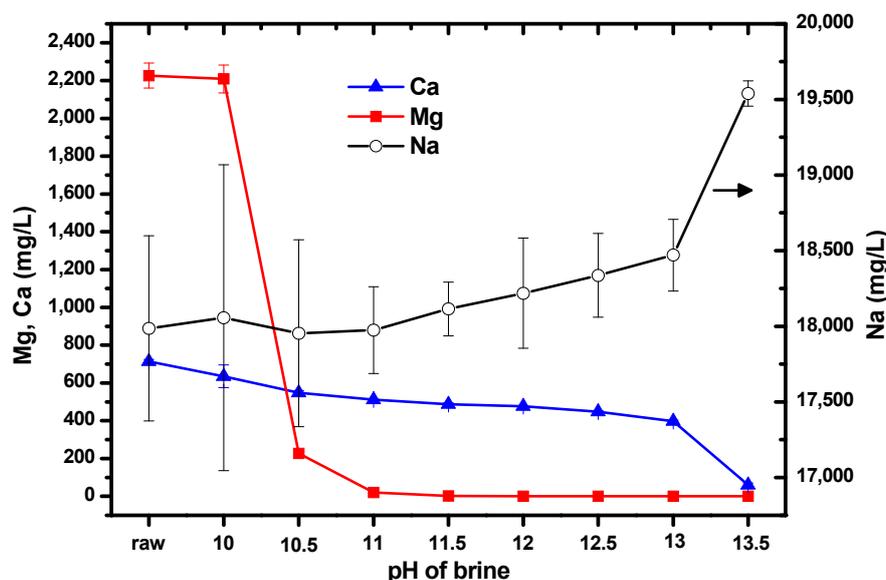
Figure 2. Concentrations of Mg, Ca, and Na as the pH of brine was increased by the addition of NaOH solution. Error bars represent one standard deviation.

It is likely that as the measured concentrations of Mg and Ca decreased as NaOH was added to the brine, the Mg and Ca ions had formed their hydroxides. If a brine suspension with a specific pH resulted in a substantial reduction in the concentration of one ion, it would strongly suggest that this was the optimal pH for isolating Mg and Ca from each other.

CO_2 mineralization is an ionic reaction between CO_3^{2-} and (divalent) metal ions. CO_2 will change its form depending on the pH environment it is exposed to, as shown in the middle column of Table 2. Therefore, increasing the pH is essential when attempting to enhance the transformation of injected gaseous CO_2 into its ionic form, CO_3^{2-}. The pH can be increased by the addition of alkaline

agents, which will dissolve and yield OH^- in aqueous solutions. If a reactant contains metal ions, metal hydroxide particles will precipitate after reaction with existing OH^-. Consequently, there is an increase in pH results in the formation of metal hydroxides and ionization of CO_2. This is the reason that addition of NaOH is required.

Table 2. Forms of CO_2 varied at pH changes and their reactions with divalent ions.

pH	Forms of CO_2	Ion Reactions
Less than neutral (~<6.35)	$CO_2 + H_2O \rightarrow H_2CO_3$	$H_2CO_3 + H_2O + M^{2+} \rightarrow H_2CO_3 + H_2O + M^{2+}$
Neutral to weak alkali	$H_2CO_3 + OH^- \rightarrow HCO_3^- + H_2O$ (pKa$_1$ = 6.4)	$2HCO_3^- + 2H_2O + 2M^{2+} \rightarrow M(HCO_3)_2 \downarrow + 2H_2O + M^{2+}$
Strong alkali (~10.33<)	$HCO_3^- + OH^- \rightarrow CO_3^{2-} + H_2O$ (pKa$_2$ = 10.2)	$2CO_3^{2-} + 2H_2O + 2M^{2+} \rightarrow 2MCO_3 \downarrow + 2H_2O$

M^{2+} represents divalent ions such as Mg^{2+} or Ca^{2+}.

When the pH was increased from 10 to 10.5, the concentration of Mg decreased by approximately 2000 mg/L, and when the pH was increased to 11, the concentration decreased by a further 180 mg/L. After this, the Mg concentration remained relatively constant up to pH 13.5. The concentration of Ca did not change significantly as the pH was varied. Consequently, we chose pH 10.5, to allow Mg from brine to form $Mg(OH)_2$ without significantly altering the concentration of Ca. Relatively pure $Mg(OH)_2$ can facilitate the production of pure Mg-carbonated particles by CO_2 injection. This is the reason for the separation or isolation of Mg and Ca from each other by pH adjustment before CO_2 injection.

We used the equations below by calculating the ion selectivity of Mg and Ca in hydroxide salts at pH 10.5 and 11.

$$\text{Precipitated ratio of an ion} = 1 - \frac{\text{measured ion concentration at a given pH}}{\text{measured ion concentration in untreated brine}} \quad (1)$$

According to Equation (1), at pH 10.5, 90% of Mg and 23% of Ca in brine precipitated as their hydroxides. As the pH was increased to 11, 99% of Mg and 29% of Ca had formed their hydroxides. Equation (1) seems to indicate that pH 11 would be more favorable for the recovery of Mg and Ca from brine. However, the precipitated ratio does not give enough information to allow a useful pH for the separation of Mg and Ca to be selected: in this study, CO_2 mineralization requires relatively pure Mg- and Ca-hydroxides to ensure that pure carbonated particles are obtained.

$$\text{Ion selectivity} = \frac{\text{measured ion concentration at a give pH}}{\text{precipitated Mg and Ca concentrations at a given pH}} \quad (2)$$

Equation (2) shows that at pH 10.5, the precipitated particles were composed of 92.3% $Mg(OH)_2$ and 7.70% $Ca(OH)_2$. Meanwhile, at pH 11, the precipitated particles were composed of 91.5% $Mg(OH)_2$ and 8.50% $Ca(OH)_2$. Therefore, the $Mg(OH)_2$ obtained was purer at pH 10.5. In addition, adjusting the pH to 10.5 required 36.1 ± 0.5 mL of 1 M NaOH solution for 0.25 L brine, while adjusting to pH 11 required 42.0 ± 0.6 mL of 1 M NaOH solution. Therefore, increasing the pH from 10.5 to 11 required an additional 5.90 mL of NaOH solution: this would increase the operational cost for the process.

3.2. Bubbling CO_2 through a Suspension at pH 10.5

CO_2 mineralization was performed by bubbling CO_2 microbubbles through a brine suspension at pH 10.5. In our previous studies on the precipitation of $CaCO_3$ by CO_2 mineralization, we found that as the pH of the suspension of $Ca(OH)_2$ into which CO_2 was injected approached neutral, all the particles had formed $CaCO_3$, leading us to regard this as the end of the reaction. We therefore discontinued CO_2 injection at this point [7,26]. On the basis of this experience, we initially intended to stop CO_2 injection when the pH of the brine approached neutral. However, in contrast to our previous experiments, we found that no particles were suspended at this neutral pH. We therefore decided to

stop CO_2 injection at a higher pH of 8. CO_2 at 600 mL/min was injected for 4.5, 5, 7, 9 mins for four experimental cycles.

The concentrations of Mg, Ca, and Na in the suspension were measured at the end of each step in the cycle shown in Figure 1. The measured results are shown in Figure 3, and the concentrations of the ions in the raw, untreated brine are given for comparison. It can be seen that the concentrations of Mg and Ca decreased during the cycles, while the concentration of Na increased owing to the addition of NaOH solution. Filtration was used to collect the particles after the CO_2 bubbling step in each cycle.
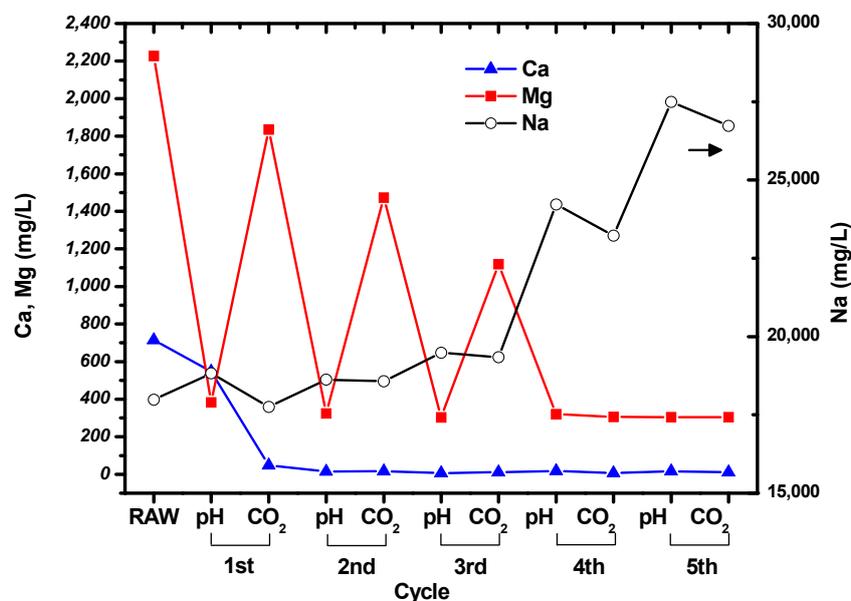
Figure 3. Changes in the concentrations of Mg, Ca, and Na during the cycles shown in Figure 1.

The concentration of Ca decreased to tens of mg/L after the first cycle, and then remained constant. This indicates that all the Ca in the brine had precipitated. Interestingly, the concentrations of Mg fluctuated during the cycles. The concentration of Mg in the suspension decreased when the pH was increased to 10.5, and then increased as CO_2 was bubbled through the brine. The Mg concentration at pH 10.5 remained constant at around ~300 mg/L, while the concentration after CO_2 bubbling decreased as the number of cycles increased. It seems that precipitation of carbonated Mg particles was less favorable than precipitation of carbonated Ca particles. However, it can be seen from the Mg and Ca concentrations measured after CO_2 bubbling that Mg carbonate precipitated during the cycles. No particles were formed after increasing the pH and bubbling CO_2 through the solution during the fifth cycle.

Based on the brine that we used, 10 million tons of brine contains 22,260 tons of Mg and 7140 tons of Ca. If assume that Mg and Ca precipitate as $MgCO_3$ and $CaCO_3$, each ion ideally reacts with 40,306 and 7854 tons of CO_2. According to the measured concentration of remained Mg and Ca in brine after the fourth cycle, 19,260 and 7080 tons of Mg and Ca react with 34,874 and 7788 tons of CO_2, respectively. The estimated amount of $MgCO_3$ and $CaCO_3$ are 66,816 and 17,700 tons by CO_2 mineralization.

3.3. Characterization of Suspended Particles from CO_2 Mineralization

After each pH increasing/CO_2-bubbling cycle, the particles in the suspensions were collected via filtration and characterized. It should be noted that too few particles were formed during the first cycle for full characterization to be carried out.

Figure 4 shows the XRD results. As depicted in the figure, the particles collected from the first cycle consisted of calcite and halite. In addition, some aragonite had crystallized owing to the coexistence of Mg and Ca ions [28]. The $CaCO_3$ successfully precipitated from the non-synthesized

brine during CO_2 mineralization. However, particles collected from other cycles could not be identified positively by standard Joint Committee on Powder Diffraction Standards (JCPDS). Only halite phase was identified. As the number of cycles increased, the halite signal became more intense.

Mg carbonates have been reported to form many crystal phases, depending on the conditions such as pressure, temperature, water content, and agitation of the reactant liquid phase [29–32]. We utilized other analytical methods that would provide information regarding the presence of Mg carbonates in the particles.
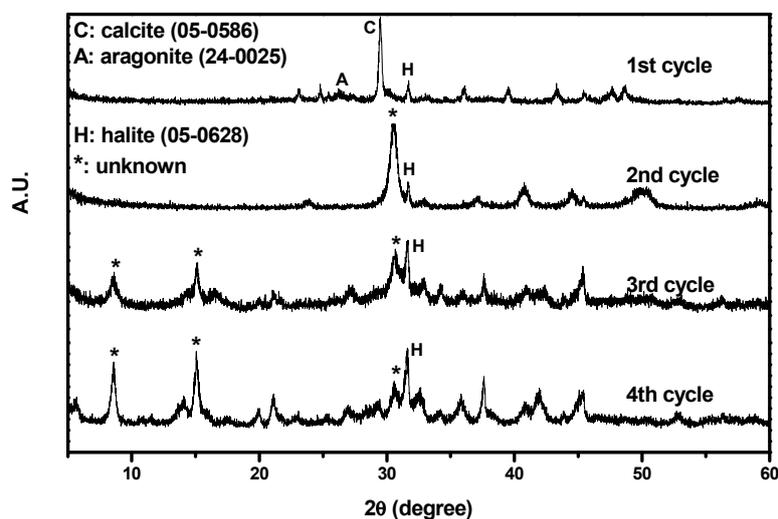
Figure 4. XRD results of the particles collected from the first to fourth cycles.

Elemental mapping by SEM-EDS revealed that the particles from the second, third, and fourth cycles consisted of Ca and Mg carbonates (Figure 5). This shows that the Mg formed carbonates, despite the fact that the precipitation of Mg carbonates is less favorable than the precipitation of Ca carbonates because Mg carbonates are more soluble than Ca carbonates and hydrated Mg ions possess more energy [33]. Figure 5 shows that the elemental distributions of Ca, Mg, C, and O were broadly similar. The second cycle produced Ca carbonate, while the third and fourth cycles produced Mg carbonate. The samples were prepared on silicon wafers to prevent the appearance of the carbon signal from the commonly used carbon adhesive tape.

The particles were also subjected to FTIR analysis; the results are shown in Figure 6. The particles that precipitated during the second cycle showed FTIR absorption bands at 727, 873, and 1406 cm^{-1}. Several research papers that identified Mg carbonates using FTIR analysis suggest that the peak at 727 cm^{-1} was likely caused by the presence $CaCO_3$ in the structure. Long et al. [34] reported that peaks at 724, 726, and 730 cm^{-1} were obtained from calcite particles including 30 mol% Mg. Similarly, Gunasekaran et al. [34,35] and Xu and Poduska [36] reported dolomite peaks at 729 and 730 cm^{-1}, respectively. These peaks arose from CO_3^{2-}. Consequently, it is possible to assign the IR peak at 727 cm^{-1} to Mg carbonates. In addition, the peaks at 873 and 1406 cm^{-1} were from the CO_3^{2-} ions in $CaCO_3$ [35,37], which was already known to be present due to XRD analysis.

The particles obtained after the third and fourth cycles both showed peaks at 852 and 877 cm^{-1}. In these cycles, both Ca and Mg carbonates formed. The peak at 852 cm^{-1} was due to calcite that included Mg. Long et al. [34] reported that calcite including Mg at 20 and 39 mol% absorbed IR at 852 cm^{-1}. CO_3^{2-} ions in dolomite also absorbed IR near this position, at 853 cm^{-1}. Meanwhile, the peak at 877 cm^{-1} indicates the presence of $CaCO_3$ [35,36,38–40]. Although we expected that the third and fourth cycles would produce Mg carbonates that excluded Ca, some of the Ca remaining in the suspension after the second cycle managed to participate in the carbonation of Mg. The peaks at 1418 and 1479 cm^{-1} are typical absorption peaks of hydromagnesite. In addition, the peak at

$3647 \ cm^{-1}$ provides further evidence of the presence of hydromagnesite. Mg from brine successfully precipitated as hydromagnesite, indicating that brine could be a useful resource for CO_2 mineralization.
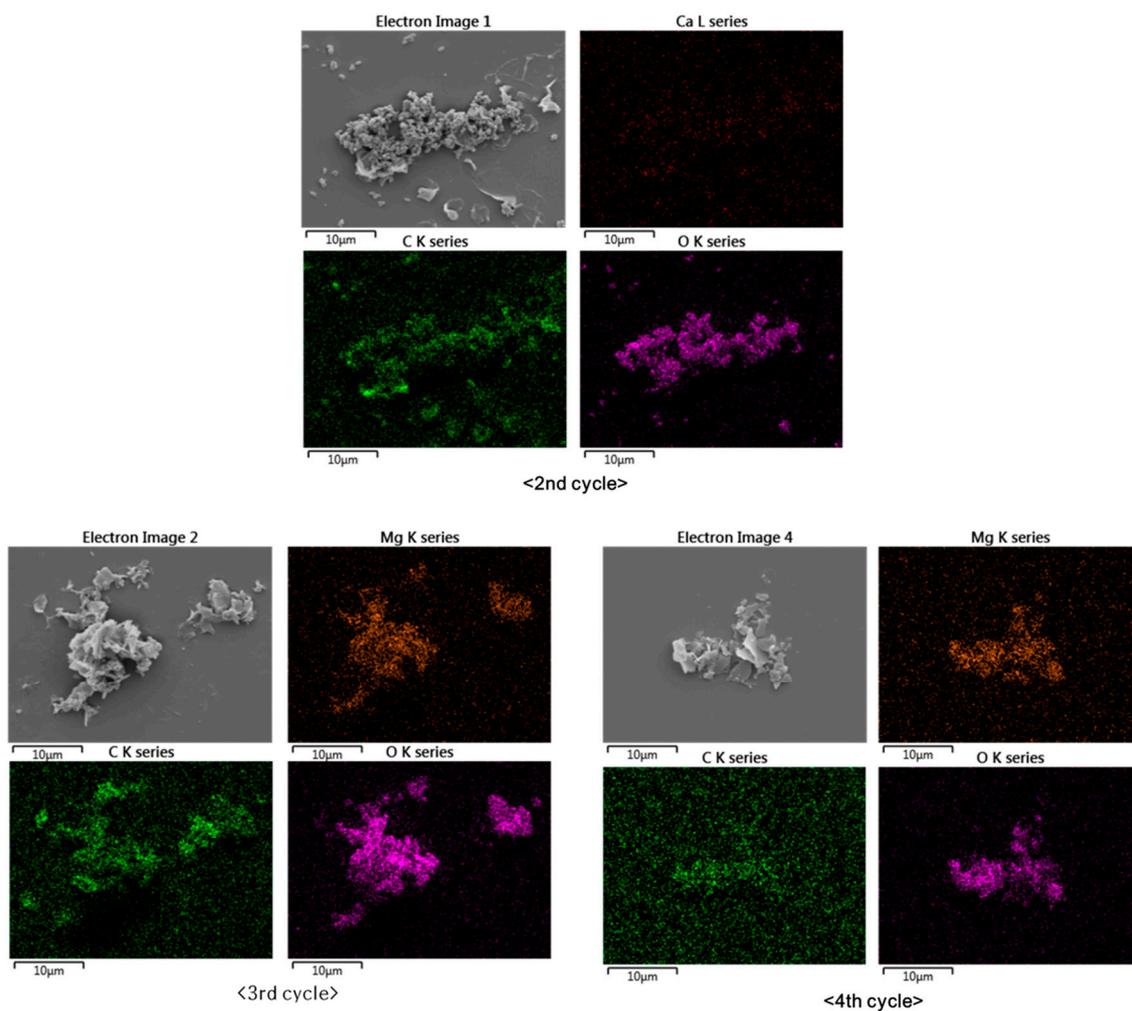
Figure 5. Elemental distributions of Mg, Ca, C, and O in particles produced during the experimental cycles.
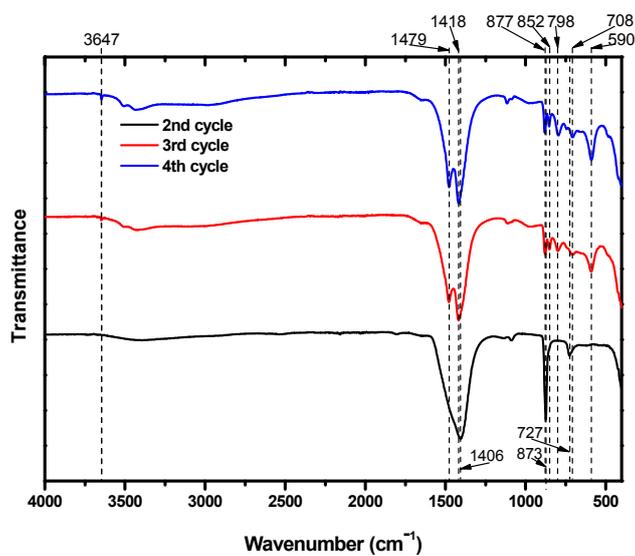
Figure 6. FTIR spectra of particles from the second, third, and fourth carbonation cycles.

　　　　In addition, characterization by TGA was used to confirm the presence of hydromagnesite. The weight losses of the particles we obtained, shown in Figure 7a, were compared with those of commercial $Mg(OH)_2$, $CaCO_3$, $MgCO_3$, and NaCl, which are shown in Figure 7b. Weight loss due to $Mg(OH)_2$ occurred between 328 and 422 °C. Losses at 589–778 °C and 180–524 °C were due to $CaCO_3$ and hydromagnesite, respectively. By comparing Figure 7a,b, it can be seen that the particles from the second cycle were composed of $Mg(OH)_2$ and $CaCO_3$. A small amount of NaCl was included in all the particles, as shown by the weight losses that began at 810 °C. The TGA curves of the particles from the third and fourth cycles were quite different from that obtained for the particles from the second cycle. The weight losses at ~450 °C in the curves of the particles from the third and fourth cycles did not quite match with what would be expected for the loss of hydromagnesite. Montes-Hermandez et al. [41] synthesized hydromagnesite and characterized particles of it using TGA. They found that hydromagnesite exhibited weight loss at 450 °C with some fluctuation at around 375 °C, which precisely matched the results shown for the particles from the third and fourth cycles in Figure 7a. There were also some differences between the TGA curves obtained for the particles from the third and fourth cycles. The curve for cycle three indicated an additional weight loss of 4.5% in the range of 635–665 °C, which indicates the coexistence of calcite and hydromagnesite. As the number of cycles increased, the purity of the hydromagnesite that precipitated increased.
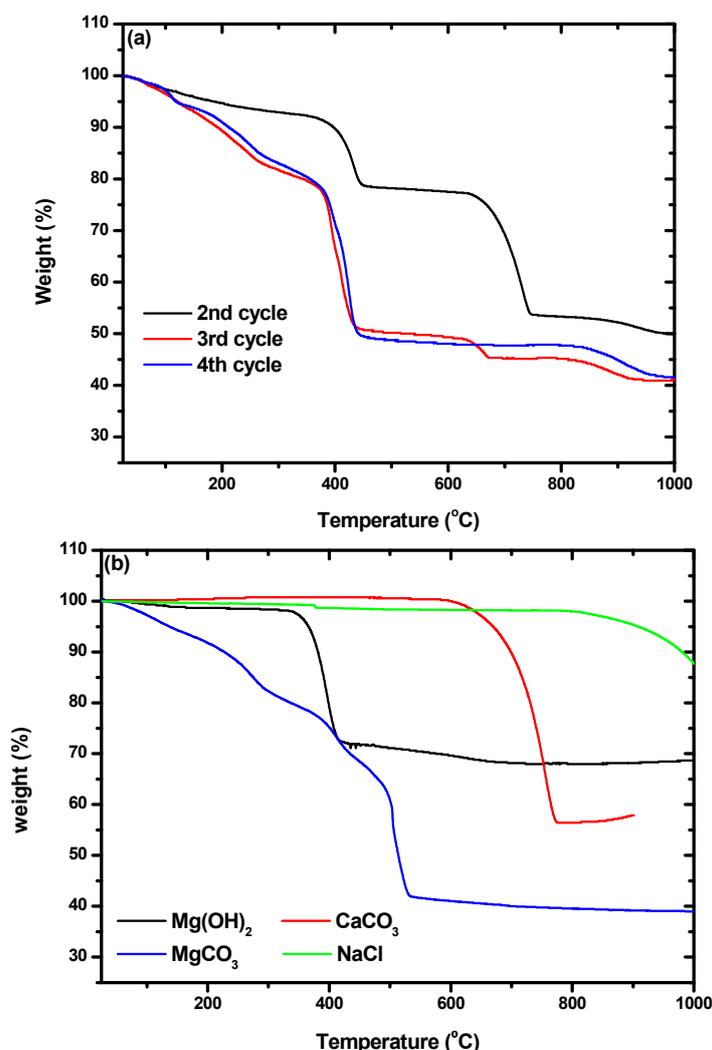
Figure 7. Thermogravimetric analysis (TGA) curves of (**a**) the precipitates obtained from the second, third, and fourth cycles; and (**b**) the commercial reagents of $Mg(OH)_2$, $MgCO_3$, $CaCO_3$, and NaCl.

4. Conclusions

Non-synthesized brine from a functional RO seawater desalination plant was used for CO_2 mineralization to fix CO_2 under ambient temperature and pressure. To the best of our knowledge, this is the first time that non-synthesized brine has been used for CO_2 mineralization. Cycles consisting of an increase in pH followed by CO_2 injection and finally filtration precipitated 99% of Ca and 86% of Mg from the brine, using them to fix CO_2 in the form of carbonated minerals. CO_2 was successfully mineralized with Ca to yield $CaCO_3$ and with Mg to produce hydromagnesite. This was shown by the characterization of the precipitates obtained from the cycles by XRD, SEM-EDS, FTIR, and TGA-DTA.

It was thought that co-presence of Ca with Mg was not favorable for the precipitation of Mg carbonates. In this study, we precipitated hydromagnesite followed by precipitation of calcite from brine. This means that the concentrations of Mg and Ca in brine are twice those in influent seawater, making it a good source of divalent ions for CO_2 mineralization. According to our experiments, 42,662 tons of CO_2 could be sequestered from 10 million tons of the brine used for a year. Moreover, 17,700 tons of $CaCO_3$ and 66,816 tons of $MgCO_3$ would be obtained.

Author Contributions: Jun-Hwan Bang and Soochun Chae conceived and designed the experiments; Yeongsuk Yoo, Seung-Woo Lee and Kyungsun Song performed experiments and analyzed the data; Jun-Hwan Bang wrote the paper.

Conflicts of Interest: The authors declare no conflict of interest.

References

1. Ko, D.-H. *Drought Causes Water Shortage Crisis in Southern Korea*; The Korea Times: Seoul, Korea, 2017.
2. Papapetrou, M.; Cipollina, A.; la Commare, U.; Micale, G.; Zaragoza, G.; Kosmadakis, G. Assessment of methodologies and data used to calculate desalination costs. *Desalination* **2017**, *419*, 8–19. [CrossRef]
3. Charcosset, C. A review of membrane processes and renewable energies for desalination. *Desalination* **2009**, *245*, 214–231. [CrossRef]
4. Alkhudhiri, A.; Darwish, N.; Hilal, N. Membrane distillation: A comprehensive review. *Desalination* **2012**, *287*, 2–18. [CrossRef]
5. Piyadasa, C.; Ridgway, H.F.; Yeager, T.R.; Stewart, M.B.; Pelekani, C.; Gray, S.R.; Orbell, J.D. The application of electromagnetic fields to the control of the scaling and biofouling of reverse osmosis membranes—A review. *Desalination* **2017**, *418*, 19–34. [CrossRef]
6. Sanna, A.; Uibu, M.; Caramanna, G.; Kuusik, R.; Maroto-Valer, M.M. A review of mineral carbonation technologies to sequester CO_2. *Chem. Soc. Rev.* **2014**, *43*, 8049–8080. [CrossRef] [PubMed]
7. Bang, J.-H.; Kim, W.; Song, K.S.; Jeon, C.W.; Chae, S.C.; Cho, H.-J.; Jang, Y.N.; Park, S.-J. Effect of experimental parameters on the carbonate mineralization with $CaSO_4 \cdot 2H_2O$ using CO_2 microbubbles. *Chem. Eng. J.* **2014**, *244*, 282–287. [CrossRef]
8. Druckenmiller, M.L.; Maroto-Valer, M.M. Carbon sequestration using brine of adjusted pH to form mineral carbonates. *Fuel Process. Technol.* **2005**, *86*, 1599–1614. [CrossRef]
9. Dri, M.; Sanna, A.; Maroto-Valer, M.M. Mineral carbonation from metal wastes: Effect of solid to liquid ratio on the efficiency and characterization of carbonated products. *Appl. Energy* **2014**, *113*, 515–523. [CrossRef]
10. Zevenhoven, R.; Wiklund, A.; Fagerlund, J.; Eloneva, S.; Veen, B.I.; Geerlings, H.; van Mossel, G.; Boerrigter, H. Carbonation of calcium-containing mineral and industrial by-products. *Front. Chem. Eng. China* **2010**, *4*, 110–119. [CrossRef]
11. Baciocchi, R.; Costa, G.; di Bartolomeo, E.; Polettini, A.; Pomi, R. The effects of accelerated carbonation on CO_2 uptake and metal release from incineration APC residues. *Waste Manag.* **2009**, *29*, 2994–3003. [CrossRef] [PubMed]
12. Baciocchi, R.; Costa, G.; Lategano, E.; Marini, C.; Polettini, A.; Pomi, R.; Postorino, P.; Rocca, S. Accelerated carbonation of different size fractions of bottom ash from RDF incineration. *Waste Manag.* **2010**, *30*, 1310–1317. [CrossRef] [PubMed]

13. Bang, J.-H.; Lee, S.-W.; Jeon, C.; Park, S.; Song, K.; Jo, W.; Chae, S. Leaching of Metal Ions from Blast Furnace Slag by Using Aqua Regia for CO_2 Mineralization. *Energies* **2016**, *9*, 996. [CrossRef]

14. Pan, S.-Y.; Chang, E.; Chiang, P.-C. CO_2 capture by accelerated carbonation of alkaline wastes: A review on its principles and applications. *Aerosol Air Qual. Res.* **2012**, *12*, 770–791. [CrossRef]

15. Bałdyga, J.; Henczka, M.; Sokolnicka, K. Utilization of carbon dioxide by chemically accelerated mineral carbonation. *Mater. Lett.* **2010**, *64*, 702–704. [CrossRef]

16. Lee, S.; Kim, J.-W.; Chae, S.; Bang, J.-H.; Lee, S.-W. CO_2 sequestration technology through mineral carbonation: An extraction and carbonation of blast slag. *J. CO_2 Util.* **2016**, *16*, 336–345. [CrossRef]

17. Soong, Y.; Fauth, D.L.; Howard, B.H.; Jones, J.R.; Harrison, D.K.; Goodman, A.L.; Gray, M.L.; Frommell, E.A. CO_2 sequestration with brine solution and fly ashes. *Energy Convers. Manag.* **2006**, *47*, 1676–1685. [CrossRef]

18. Li, P.; Pan, S.-Y.; Pei, S.; Lin, Y.J.; Chiang, P.-C. Challenges and perspectives on carbon fixation and utilization technologies: An overview. *Aerosol Air Qual. Res.* **2016**, *16*, 1327–1344. [CrossRef]

19. Shenvi, S.S.; Isloor, A.M.; Ismail, A.F. A review on RO membrane technology: Developments and challenges. *Desalination* **2015**, *368*, 10–26. [CrossRef]

20. Morrison, J.; Jauffret, G.; Galvez-Martos, J.L.; Glasser, F.P. Magnesium-based cements for CO_2 capture and utilisation. *Cem. Concr. Res.* **2016**, *85*, 183–191. [CrossRef]

21. Liu, Q.; Maroto-Valer, M.M. Studies of pH buffer systems to promote carbonate formation for CO_2 sequestration in brines. *Fuel Process. Technol.* **2012**, *9*, 6–13. [CrossRef]

22. Wang, W.; Liu, X.; Wang, P.; Zheng, Y.; Wang, M. Enhancement of CO_2 Mineralization in Ca^{2+}-/Mg^{2+}-Rich Aqueous Solutions Using Insoluble Amine. *Ind. Eng. Chem. Res.* **2013**, *52*, 8028–8033. [CrossRef]

23. Xie, H.; Liu, T.; Hou, Z.; Wang, Y.; Wang, J.; Tang, L.; Jiang, W.; He, Y. Using electrochemical process to mineralize CO_2 and separate Ca^{2+}/Mg^{2+} ions from hard water to produce high value-added carbonates. *Environ. Earth Sci.* **2015**, *73*, 6881–6890. [CrossRef]

24. Langmuir, D. Stability of Carbonates in the System MgO-CO_2-H_2O. *J. Geol.* **1965**, *73*, 730–754. [CrossRef]

25. Lide, D.R. *CRC Handbook of Chemistry and Physics*; CRC Press: Boca Raton, FL, USA, 1997.

26. Bang, J.-H.; Jang, Y.N.; Kim, W.; Song, K.S.; Jeon, C.W.; Chae, S.C.; Lee, S.-W.; Park, S.-J.; Lee, M.G. Precipitation of calcium carbonate by carbon dioxide microbubbles. *Chem. Eng. J.* **2011**, *174*, 413–420. [CrossRef]

27. Bang, J.-H.; Song, K.; Park, S.; Jeon, C.; Lee, S.-W.; Kim, W. Effects of CO_2 Bubble Size, CO_2 Flow Rate and Calcium Source on the Size and Specific Surface Area of $CaCO_3$ Particles. *Energies* **2015**, *8*, 12304. [CrossRef]

28. Santos, R.M.; Bodor, M.; Dragomir, P.N.; Vraciu, A.G.; Vlad, M.; van Gerven, T. Magnesium chloride as a leaching and aragonite-promoting self-regenerative additive for the mineral carbonation of calcium-rich materials. *Miner. Eng.* **2014**, *59*, 71–81. [CrossRef]

29. Cheng, W.; Li, Z. Nucleation kinetics of nesquehonite ($MgCO_3 \cdot 3H_2O$) in the $MgCl_2$-Na_2CO_3 system. *J. Cryst. Growth* **2010**, *312*, 1563–1571. [CrossRef]

30. Hales, M.C.; Frost, R.L.; Martens, W.N. Thermo-Raman spectroscopy of synthetic nesquehonite —Implication for the geosequestration of greenhouse gases. *J. Raman Spectrosc.* **2008**, *39*, 1141–1149. [CrossRef]

31. Coleyshaw, E.E.; Crump, G.; Griffith, W.P. Vibrational spectra of the hydrated carbonate minerals ikaite, monohydrocalcite, lansfordite and nesquehonite. *Spectrochim. Acta Part A Mol. Biomolecul. Spectroscop.* **2003**, *59*, 2231–2239. [CrossRef]

32. Hopkinson, L.; Kristova, P.; Rutt, K.; Cressey, G. Phase transitions in the system MgO–CO_2–H_2O during CO_2 degassing of Mg-bearing solutions. *Geochim. Cosmochim. Acta* **2012**, *76*, 1–13. [CrossRef]

33. Xu, J.; Yan, C.; Zhang, F.; Konishi, H.; Xu, H.; Teng, H.H. Testing the cation-hydration effect on the crystallization of Ca–Mg–CO_3 systems. *Proc. Natl. Acad. Sci. USA* **2013**, *110*, 17750–17755. [CrossRef] [PubMed]

34. Long, X.; Nasse, M.J.; Ma, Y.; Qi, L. From synthetic to biogenic Mg-containing calcites: A comparative study using FTIR microspectroscopy. *Phys. Chem. Chem. Phys.* **2012**, *14*, 2255–2263. [CrossRef] [PubMed]

35. Gunasekaran, S.; Anbalagan, G.; Pandi, S. Raman and infrared spectra of carbonates of calcite structure. *J. Raman Spectrosc.* **2006**, *37*, 892–899. [CrossRef]

36. Xu, B.; Poduska, K.M. Linking crystal structure with temperature-sensitive vibrational modes in calcium carbonate minerals. *Phys. Chem. Chem. Phys.* **2014**, *16*, 17634–17639. [CrossRef] [PubMed]

37. Pandey, S.; Sengupta, J. Fourier transform infrared spectroscopy: A tool for detection of lime content in hot mix asphalt. In Proceedings of the 26th ARRB Conference, Sydney, Australia, 19–22 October 2014; p. 11.

38. Bourrata, X.; Qiao, L.; Feng, Q.; Angellier, M.; Dissaux, A.; Beny, J.-M.; Barbin, V.; Stempflé, P.; Rousseau, M.; Lopez, E. Origin of growth defects in pearl. *Mater. Charact.* **2012**, *72*, 94–103. [CrossRef]

39. Junfeng, J.; Yun, G.; Balsam, W.; Damuth, J.E.; Jun, C. Rapid identification of dolomite using a Fourier transform infrared spectrophotometer (FTIR): A fast method for identifying Heinrich events in IODP Site U1308. *Mar. Geol.* **2009**, *258*, 60.

40. Bang, J.-H.; Song, K.S.; Lee, M.G.; Jeon, C.W.; Jang, Y.N. Effect of Critical Micelle Concentration of Sodium Dodecyl Sulfate Dissolved in Calcium and Carbonate Source Solutions on Characteristics of Calcium Carbonate Crystals. *Mater. Trans.* **2010**, *51*, 1486–1489. [CrossRef]

41. Montes-Hernandez, G.; Renard, F.; Chiriac, R.; Findling, N.; Toche, F. Rapid Precipitation of Magnesite Microcrystals from $Mg(OH)_2$-H_2O-CO_2 Slurry Enhanced by NaOH and a Heat-Aging Step (from ~20 to 90 °C). *Cryst. Growth Des.* **2012**, *12*, 5233–5240. [CrossRef]